Effective 2HDM Yukawa Interactions and a Strong First-Order Electroweak Phase Transition

Anisha,[a] **Duarte Azevedo,**[b] **Lisa Biermann,**[b] **Christoph Englert,**[a] **and Margarete Mühlleitner**[b]

[a]*School of Physics & Astronomy, University of Glasgow, Glasgow G12 8QQ, United Kingdom*

[b]*Institute for Theoretical Physics, Karlsruhe Institute of Technology, 76128 Karlsruhe, Germany*

E-mail: anisha@glasgow.ac.uk, duarte.azevedo@kit.edu, lisa.biermann@kit.edu, christoph.englert@glasgow.ac.uk, margarete.muehlleitner@kit.edu

ABSTRACT: The top quark as the heaviest particle in the Standard Model (SM) defines an important mass scale for Higgs physics and the electroweak scale itself. It is therefore a well-motivated degree of freedom which could reveal the presence of new interactions beyond the SM. Correlating modifications of the top-Higgs interactions in the 2-Higgs-Doublet Model (2HDM), we analyse effective field theory deformations of these interactions from the point of view of a strong first-order electroweak phase transition (SFOEWPT). We show that such modifications are compatible with current Higgs data and that an SFOEWPT can be tantamount to a current overestimate of exotic Higgs searches' sensitivity at the LHC in $t\bar{t}$ and four top quark final states. We argue that these searches remain robust from the point of accidental signal-background interference so that the current experimental strategy might well lead to 2HDM-like discoveries in the near future.

Contents

1 Introduction

The lack of direct evidence for new interactions beyond the Standard Model (BSM) at the Large Hadron Collider (LHC) and other experiments is puzzling given the theoretically and experimentally established need to go beyond the Standard Model (SM). As experiments are moving increasingly towards model-independent methods to report measurements and BSM sensitivity, a range of established BSM phenomena continue to signpost particular sectors of the SM for further phenomenological scrutiny. One such sector is related to the interactions of the top quark. The top quark, as the heaviest believed-fundamental particle enters a range of phenomenologically accessible final states at the LHC. It decays before hadronisation thus enabling the direct analysis of its properties, whilst abundantly produced in hadronic collisions. Furthermore, it creates a large radiative pull of electroweak interactions, which is highlighted by the sensitivity of the electroweak fit to the top mass [1], the metastability of the electroweak vacuum at high scales [2, 3], as well as, its role as a threshold in Higgs physics (e.g. [4, 5]). It might be fair to say that the "right" theory of BSM interactions seems further away from discovery than ever, but the top quark and its relation to the weak scale might well hold the key to unlocking the secrets of electroweak symmetry breaking.[1]

The critical role of the top quark is apparent from its strong coupling to the Higgs field with a Yukawa interaction of order unity in the SM. The qualitative pattern predicted by the SM has been spectacularly validated by the discovery of the Higgs boson in $H \to \gamma\gamma$ decays with direct evidence from top-associated Higgs production providing mounting evidence of the SM-like character of top-Higgs interactions, alluding to fundamental mass generation for the top quark through the

---

[1]This is echoed by the central part that the top plays in concrete models of BSM physics, ranging from supersymmetry to strongly interacting models.

electroweak vacuum. This relation also puts the top quark centre-stage for the emergence of the non-trivial vacuum itself in the early history of our Universe, potentially playing *the* critical role in facilitating a strong first-order electroweak phase transition (SFOEWPT) in the context of electroweak baryogenesis to address the Sakharov criteria [6] for matter anti-matter asymmetry. Additional sources of CP violation (under the assumption that baryogenesis proceeds canonically) could be traceable into phases of the Yukawa interactions (for recent phenomenological analyses see Refs. [7–9]), and their appearance is indicative of a richer scalar sector such as the 2-Higgs-Doublet Model (2HDM) [10–13]. To this end, in this work, we focus on the possibility of obtaining an SFOEWPT in the 2HDM with a specific focus on the role of the top quark. The characteristics of additional SFOEWPT-relevant contributions in the scalar sector have been discussed in Refs. [14], highlighting a qualitative agreement with similar discussions in the context of the SM: Additional Higgs interactions that lead to an SFOEWPT show up predominantly as modifications of Higgs pair interactions via modifications of the Higgs self-coupling. Following the canonical arguments of thermodynamics, such modifications should predominantly be visible in the phenomenology of the light degrees of freedom, in agreement with the findings of Ref. [14]. In flavon extensions of the SM, it has been observed that large Yukawa coupling modifications can lead to the desired SFOEWPT [15]. When these effects are captured by the top quark modifications, this can lead to large departures from the expected phenomenology of the BSM states.

In this paper, we consider a motivated effective field theory (EFT) extension of the top quark sector in the 2HDM. On the one hand, this addresses the emerging tension of observing an SFOEWPT in the 2HDM of type II given the current Higgs coupling measurements [16–19]; on the other hand the means of EFT enable us to remain agnostic to the particular extension of the 2HDM.[2]

This paper is organised as follows: Section 2 gives an overview of the 2HDM type II and its EFT extension relevant to this work. Section 3 details the relevance of these modifications for an SFOEWPT which is backed up by a comprehensive scan over the 2HDM's type II EFT extension. As these results are relevant for the phenomenology programme at the LHC, we perform a detailed analysis of the EFT modifications for Higgs physics as a function of an SFOEWPT in Sec. 4.2. We conclude in Sec. 5.

2 The 2HDM and its Dimension-6 Yukawa Extension

We start our discussion with the canonical 2HDM dimension-4 Yukawa terms which are given by by [27, 28]

$$\mathcal{L}_{\text{Yuk}}^{\text{dim-4}} = -Y_1^e \bar{L}\Phi_1 e - Y_2^e \bar{L}\Phi_2 e - Y_1^d \bar{Q}\Phi_1 d - Y_2^d \bar{Q}\Phi_2 d - Y_1^u \bar{Q}\tilde{\Phi}_1 u - Y_2^u \bar{Q}\tilde{\Phi}_2 u + \text{h.c.}\,, \qquad (2.1)$$

where $\Phi_{1,2}$ are $SU(2)_L$ doublets with hypercharge $Y = 1$. The two doublets are expanded as

$$\Phi_1 = \begin{pmatrix} \phi_1^+ \\ \frac{1}{\sqrt{2}}(v_1 + \zeta_1 + i\psi_1) \end{pmatrix}, \qquad \Phi_2 = \begin{pmatrix} \phi_2^+ \\ \frac{1}{\sqrt{2}}(v_2 + \zeta_2 + i\psi_2) \end{pmatrix}. \qquad (2.2)$$

---

[2]Employing matching computations [20–25], results can then be connected to concrete UV extensions of the 2HDM. We will not discuss this further in this work. It is furthermore worth noting that considering non-SM degrees as dynamical rather than turning directly to SMEFT is particularly motivated given the limitations that SMEFT faces when considering electroweak phase transitions [26].

Here, v_1 and v_2 are the vacuum expectation value (vev) of Φ_1 and Φ_2, respectively, with $v_1^2 + v_2^2 = v^2$ and $v \simeq 246$ GeV. The ϕ_i^+ label the charged fields and ζ_i is the neutral CP-even and ψ_i is the neutral CP-odd field for $i = 1, 2$. Motivated by the possibility of connecting the 2HDM of type II to high-scale supersymmetry, we will focus on this scenario in the following; it is also worth pointing out that the 2HDM of type I does not face comparable tension as the 2HDM when considered from the perspective of an SFOEWPT [16–18, 29]. In the type II case, the Yukawa interactions reduce to

$$\mathcal{L}_{\text{Yuk}}^{\text{dim-4}} = -Y_1^e \bar{L} \Phi_1 e - Y_1^d \bar{Q} \Phi_1 d - Y_2^u \bar{Q} \tilde{\Phi}_2 u + \text{h.c.} \,. \tag{2.3}$$

After spontaneous symmetry breaking, we have five physical fields, two CP-even neutral scalars H and h (ordered in mass to $m_H > m_h$), one CP-odd scalar A and a charged pair $H^\pm$. These fields are related to the interaction fields through the rotation matrix $R(x)$ as:

$$\begin{pmatrix} H \\ h \end{pmatrix} = R(\alpha) \begin{pmatrix} \zeta_1 \\ \zeta_2 \end{pmatrix}, \quad \begin{pmatrix} G^0 \\ A \end{pmatrix} = R(\beta) \begin{pmatrix} \psi_1 \\ \psi_2 \end{pmatrix}, \quad \begin{pmatrix} G^\pm \\ H^\pm \end{pmatrix} = R(\beta) \begin{pmatrix} \phi_1^\pm \\ \phi_2^\pm \end{pmatrix}, \tag{2.4}$$

with

$$R(x) = \begin{pmatrix} \cos x & \sin x \\ -\sin x & \cos x \end{pmatrix}. \tag{2.5}$$

The mixing angle β is also expressed as:

$$\tan \beta = \frac{v_2}{v_1}, \tag{2.6}$$

which provides the relation to $v \simeq 246$ GeV via $v_1 = v \cos \beta$ and $v_2 = v \sin \beta$. The Higgs boson couplings to fermions f in the mass basis fields are given by

$$\mathcal{L}_{\text{Yuk}}^{\text{dim-4}} = - \sum_{f=u,d,\ell} \frac{m_f}{v} \left(\xi_h^f \bar{f} f h + \xi_H^f \bar{f} f H - i \xi_A^f \bar{f} \gamma_5 f A \right)$$
$$+ \left[\frac{\sqrt{2} V_{ud}}{v} \bar{u} \left(m_d \xi_A^d P_R + m_u \xi_A^u P_L \right) d \, H^+ + \frac{\sqrt{2}}{v} m_\ell \xi_A^l (\bar{\nu} P_R \ell) H^+ + \text{h.c.} \right], \tag{2.7}$$

where $P_{L,R}$ are the left and right chirality projectors and the coupling modifiers ξ for the type II case are listed in Tab. 1. The mass-coupling relations will be modified by the dimension-6 interactions which we detail below.

Having set the stage of the renormalisable $d = 4$ part of the 2HDM, we can now turn to its EFT deformation. The extension of these Yukawa interactions to the effective dimension-6 level results

Model	ξ_h^u	$\xi_h^{d(e)}$	ξ_H^u	$\xi_H^{d(e)}$	ξ_A^u	$\xi_A^{d(e)}$
type II	$\cos\alpha / \sin\beta$	$-\sin\alpha / \cos\beta$	$\sin\alpha / \sin\beta$	$\cos\alpha / \cos\beta$	$\cot\beta$	$\tan\beta$

Table 1. Coupling modifiers ξ for 2HDM type II and up- and down-type quarks.

$O_{L\tau}^{1(21)}$	$(\bar{L}\tau\Phi_1)(\Phi_2^\dagger\Phi_1)$	$O_{L\tau}^{2(22)}$	$(\bar{L}\tau\Phi_2)(\Phi_2^\dagger\Phi_2)$	$O_{L\tau}^{2(11)}$	$(\bar{L}\tau\Phi_2)(\Phi_1^\dagger\Phi_1)$
$O_{L\tau}^{1(12)}$	$(\bar{L}\tau\Phi_1)(\Phi_1^\dagger\Phi_2)$	$O_{Qb}^{1(21)}$	$(\bar{Q}b\Phi_1)(\Phi_2^\dagger\Phi_1)$	$O_{Qb}^{2(22)}$	$(\bar{Q}b\Phi_2)(\Phi_2^\dagger\Phi_2)$
$O_{Qb}^{2(11)}$	$(\bar{Q}b\Phi_2)(\Phi_1^\dagger\Phi_1)$	$O_{Qb}^{1(12)}$	$(\bar{Q}b\Phi_1)(\Phi_1^\dagger\Phi_2)$	$O_{Qt}^{2(22)}$	$(\bar{Q}t\tilde{\Phi}_2)(\Phi_2^\dagger\Phi_2)$
$O_{Qt}^{1(12)}$	$(\bar{Q}t\tilde{\Phi}_1)(\Phi_1^\dagger\Phi_2)$	$O_{Qt}^{2(11)}$	$(\bar{Q}t\tilde{\Phi}_2)(\Phi_1^\dagger\Phi_1)$	$O_{Qt}^{1(21)}$	$(\bar{Q}t\tilde{\Phi}_1)(\Phi_2^\dagger\Phi_1)$
$O_{L\tau}^{1(11)}$	$(\bar{L}\tau\Phi_1)(\Phi_1^\dagger\Phi_1)$	$O_{L\tau}^{2(12)}$	$(\bar{L}\tau\Phi_2)(\Phi_1^\dagger\Phi_2)$	$O_{L\tau}^{1(22)}$	$(\bar{L}\tau\Phi_1)(\Phi_2^\dagger\Phi_2)$
$O_{L\tau}^{2(21)}$	$(\bar{L}\tau\Phi_2)(\Phi_2^\dagger\Phi_1)$	$O_{Qb}^{1(11)}$	$(\bar{Q}b\Phi_1)(\Phi_1^\dagger\Phi_1)$	$O_{Qb}^{2(12)}$	$(\bar{Q}b\Phi_2)(\Phi_1^\dagger\Phi_2)$
$O_{Qb}^{1(22)}$	$(\bar{Q}b\Phi_1)(\Phi_2^\dagger\Phi_2)$	$O_{Qb}^{2(21)}$	$(\bar{Q}b\Phi_2)(\Phi_2^\dagger\Phi_1)$	$O_{Qt}^{1(11)}$	$(\bar{Q}t\tilde{\Phi}_1)(\Phi_1^\dagger\Phi_1)$
$O_{Qt}^{2(21)}$	$(\bar{Q}t\tilde{\Phi}_2)(\Phi_2^\dagger\Phi_1)$	$O_{Qt}^{1(22)}$	$(\bar{Q}t\tilde{\Phi}_1)(\Phi_2^\dagger\Phi_2)$	$O_{Qt}^{2(12)}$	$(\bar{Q}t\tilde{\Phi}_2)(\Phi_1^\dagger\Phi_2)$

Table 2. Dimension-6 2HDMEFT operators of class $\Psi^2\Phi^3$. Each of these operators has a distinct Hermitian conjugate. Here, $\bar{L} = (\bar{\nu}_\tau \;\; \bar{\tau})$ and $\bar{Q} = (\bar{t} \;\; \bar{b})$. The operators coloured in magenta violate the $\mathbb{Z}_2$ symmetry.

from the class[3] $\sim \Psi^2\Phi^3$ which modifies the 2HDM Yukawa Lagrangian [31–34]

$$\mathcal{L}_{\text{EFT}} = \mathcal{L}_{\text{2HDM}} + \sum_i \frac{C_i}{\Lambda^2}O_i \quad \implies \quad \mathcal{L}_{\text{Yuk}}^{\text{EFT}} = \mathcal{L}_{\text{Yuk}}^{\text{dim-4}} + \sum_i \frac{C_i}{\Lambda^2}O_i \,. \tag{2.8}$$

Here, O_i are the dimension-6 operators and C^i are the corresponding Wilson Coefficients (WCs). For our work, we consider operators dealing with the third generation fermions i.e. τ, t, b. The structures of these operators are given explicitly in Tab. 2. For the type II scenario, the $\mathbb{Z}_2$ symmetry is enforced with the following transformations in these operators: for the τ lepton and the b quark, $\Phi_1 \to \Phi_1$ and $\Phi_2 \to -\Phi_2$ and for the t quark $\Phi_1 \to -\Phi_1$ and $\Phi_2 \to \Phi_2$. The operators violating the $\mathbb{Z}_2$ symmetry are coloured in magenta. This complete set of operators modifies the fermion mass terms and the scalar-fermions couplings.

In the broken phase, these interactions lead to corrections to the fermion masses compared to the dimension-4 mass-Yukawa coupling relation,

$$\Delta M_\Psi = -\frac{1}{2\sqrt{2}\Lambda^2}\Big[C_{Q\Psi}^{1(11)}v_1^3 + v_1^2 v_2(C_{Q\Psi}^{1(12)} + C_{Q\Psi}^{1(21)} + C_{Q\Psi}^{2(11)})$$
$$+ v_1 v_2^2(C_{Q\Psi}^{1(22)} + C_{Q\Psi}^{2(12)} + C_{Q\Psi}^{2(21)}) + C_{Q\Psi}^{2(22)}v_2^3\Big] \text{ for } \Psi \equiv \{t, b, \tau\}. \tag{2.9}$$

For the considered type II scenario, the modified third-generation fermion mass terms are then

$$M_t = \frac{v_2}{\sqrt{2}}\Big[Y_2^t - \frac{1}{2\Lambda^2}\Big(C_{Qt}^{1(11)}\frac{v_1^3}{v_2} + v_1^2(C_{Qt}^{1(12)} + C_{Qt}^{1(21)} + C_{Qt}^{2(11)})$$
$$+ v_1 v_2(C_{Qt}^{1(22)} + C_{Qt}^{2(12)} + C_{Qt}^{2(21)}) + C_{Qt}^{2(22)}v_2^2\Big)\Big], \tag{2.10a}$$
$$M_b = \frac{v_1}{\sqrt{2}}\Big[Y_1^b - \frac{1}{2\Lambda^2}\Big(C_{Qb}^{1(11)}v_1^2 + v_1 v_2(C_{Qb}^{1(12)} + C_{Qb}^{1(21)} + C_{Qb}^{2(11)})$$

---

[3]The dimension-6 effective operators for 2HDMEFT are classified into 8 classes following the convention of the Warsaw basis given in [30].

$$+ v_2^2(C_{Qb}^{1(22)} + C_{Qb}^{2(12)} + C_{Qb}^{2(21)}) + C_{Qb}^{2(22)}\frac{v_2^3}{v_1}\Big)\Big], \tag{2.10b}$$

$$M_\tau = \frac{v_1}{\sqrt{2}}\Big[Y_1^\tau - \frac{1}{2\Lambda^2}\Big(C_{L\tau}^{1(11)}v_1^2 + v_1v_2(C_{L\tau}^{1(12)} + C_{L\tau}^{1(21)} + C_{L\tau}^{2(11)})$$

$$+ v_2^2(C_{L\tau}^{1(22)} + C_{L\tau}^{2(12)} + C_{L\tau}^{2(21)}) + C_{L\tau}^{2(22)}\frac{v_2^3}{v_1}\Big)\Big]. \tag{2.10c}$$

These mass-coupling relations are different to the ones for $d = 4$ quoted in (2.7), but we recover $M = m$ for $\Lambda \to \infty$. For our work, the 2HDM dim-4 Yukawa couplings given in Eq. (2.3) are specifically for the third-generation fermions. Taking masses of fermions as the dimension-6 extended input quantities, i.e.

$$M_t = \frac{v_2}{\sqrt{2}}\mathcal{Y}_2^t, \qquad M_b = \frac{v_1}{\sqrt{2}}\mathcal{Y}_1^b, \qquad M_\tau = \frac{v_1}{\sqrt{2}}\mathcal{Y}_1^\tau, \tag{2.11}$$

the dimension-4 Yukawa couplings are redefined as

$$Y_2^t \to \mathcal{Y}_2^t + \frac{1}{2\Lambda^2}\Big(C_{Qt}^{1(11)}\frac{v_1^3}{v_2} + v_1^2(C_{Qt}^{1(12)} + C_{Qt}^{1(21)} + C_{Qt}^{2(11)}) \tag{2.12a}$$

$$+ v_1v_2(C_{Qt}^{1(22)} + C_{Qt}^{2(12)} + C_{Qt}^{2(21)}) + C_{Qt}^{2(22)}v_2^2\Big),$$

$$Y_1^b \to \mathcal{Y}_1^b + \frac{1}{2\Lambda^2}\Big(C_{Qb}^{1(11)}v_1^2 + v_1v_2(C_{Qb}^{1(12)} + C_{Qb}^{1(21)} + C_{Qb}^{2(11)}) \tag{2.12b}$$

$$+ v_2^2(C_{Qb}^{1(22)} + C_{Qb}^{2(12)} + C_{Qb}^{2(21)}) + C_{Qb}^{2(22)}\frac{v_2^3}{v_1}\Big),$$

$$Y_1^\tau \to \mathcal{Y}_1^\tau + \frac{1}{2\Lambda^2}\Big(C_{L\tau}^{1(11)}v_1^2 + v_1v_2(C_{L\tau}^{1(12)} + C_{L\tau}^{1(21)} + C_{L\tau}^{2(11)}) \tag{2.12c}$$

$$+ v_2^2(C_{L\tau}^{1(22)} + C_{L\tau}^{2(12)} + C_{L\tau}^{2(21)}) + C_{L\tau}^{2(22)}\frac{v_2^3}{v_1}\Big).$$

These replacements shift the dimension-6-induced coupling modifications into the Higgs-fermion interactions for given fermion masses; the coupling modifiers ξ mentioned in Tab. 1 get additional dimension-6 corrections. The modified scalar fermion couplings are given by (assuming $V_{tb} = 1$)

$$\xi_h^t = \frac{\cos\alpha}{\sin\beta} + \frac{v^3}{M_t}\frac{1}{\sqrt{2}\Lambda^2}\Big[-C_{Qt}^{2(22)}\cos\alpha\sin^2\beta + \frac{\cos^2\beta}{2}\Big(\frac{\cos\alpha\cos\beta}{\sin\beta} + 3\sin\alpha\Big)C_{Qt}^{1(11)}$$

$$-\frac{\sin\beta}{2}\cos(\alpha+\beta)\Big(C_{Qt}^{2(21)} + C_{Qt}^{2(12)} + C_{Qt}^{1(22)}\Big) + \cos\beta\sin\beta\sin\alpha\Big(C_{Qt}^{1(12)} + C_{Qt}^{1(21)} + C_{Qt}^{2(11)}\Big)\Big], \tag{2.13a}$$

$$\xi_H^t = \frac{\sin\alpha}{\sin\beta} + \frac{v^3}{M_t}\frac{1}{\sqrt{2}\Lambda^2}\Big[-C_{Qt}^{2(22)}\sin\alpha\sin^2\beta + \frac{\cos^2\beta}{2}\Big(\frac{\sin\alpha\cos\beta}{\sin\beta} - 3\cos\alpha\Big)C_{Qt}^{1(11)}$$

$$-\frac{\sin\alpha}{2}\sin(\alpha+\beta)\Big(C_{Qt}^{2(21)} + C_{Qt}^{2(12)} + C_{Qt}^{1(22)}\Big) - \cos\beta\sin\beta\cos\alpha\,(C_{Qt}^{1(12)} + C_{Qt}^{1(21)} + C_{Qt}^{2(11)})\Big], \tag{2.13b}$$

$$\xi_A^t = \cot\beta + \frac{v^3}{M_t}\frac{1}{\sqrt{2}\Lambda^2}\Big[\frac{\sin\beta}{2}(-C_{Qt}^{2(21)} + C_{Qt}^{2(12)} + C_{Qt}^{1(22)}) + \cos\beta\,C_{Qt}^{1(12)} + \frac{\cot\beta\cos\beta}{2}C_{Qt}^{1(11)}\Big], \tag{2.13c}$$

$$\xi_h^b = -\frac{\sin\alpha}{\cos\beta} + \frac{v^3}{M_b}\frac{1}{\sqrt{2}\Lambda^2}\Big[-C_{Qb}^{2(22)}\sin^2\beta\Big(\frac{3\cos\alpha}{2} + \frac{\sin\alpha\sin\beta}{2\cos\beta}\Big) + \sin\alpha\cos^2\beta\,C_{Qb}^{1(11)}$$

$$- 5 -$$

$$-\frac{\cos\beta}{2}\cos\left(\alpha+\beta\right)\left(C_{Qb}^{1(12)}+C_{Qb}^{1(21)}+C_{Qb}^{2(11)}\right)-\cos\alpha\cos\beta\sin\beta\,\left(C_{Qb}^{2(21)}+C_{Qb}^{2(12)}+C_{Qb}^{1(22)}\right)\Big]\,,$$
$$(2.13\text{d})$$

$$\xi_H^b = \frac{\cos\alpha}{\cos\beta}+\frac{v^3}{M_b}\frac{1}{\sqrt{2}\Lambda^2}\Big[C_{Qb}^{2(22)}\sin^2\beta\left(-\frac{3\sin\alpha}{2}+\frac{\cos\alpha\sin\beta}{2\cos\beta}\right)-\cos\alpha\cos^2\beta\,C_{Qb}^{1(11)}$$
$$-\frac{\cos\beta}{2}\sin\left(\alpha+\beta\right)\left(C_{Qb}^{1(12)}+C_{Qb}^{1(21)}+C_{Qb}^{2(11)}\right)-\sin\alpha\cos\beta\sin\beta\,\left(C_{Qb}^{2(21)}+C_{Qb}^{2(12)}+C_{Qb}^{1(22)}\right)\Big]\,,$$
$$(2.13\text{e})$$

$$\xi_A^b = \tan\beta+\frac{v^3}{M_b}\frac{1}{\sqrt{2}\Lambda^2}\Big[C_{Qb}^{2(22)}\frac{\tan\beta\sin\beta}{2}+\sin\beta\,C_{Qb}^{2(12)}+\frac{\cos\beta}{2}\left(C_{Qb}^{1(12)}-C_{Qb}^{1(21)}+C_{Qb}^{2(11)}\right)\Big]\,,$$
$$(2.13\text{f})$$

$$\xi_h^\tau = -\frac{\sin\alpha}{\cos\beta}+\frac{v^3}{M_\tau}\frac{1}{\sqrt{2}\Lambda^2}\Big[-C_{L\tau}^{2(22)}\sin^2\beta\left(\frac{3\cos\alpha}{2}+\frac{\sin\alpha\sin\beta}{2\cos\beta}\right)+\sin\alpha\cos^2\beta\,C_{L\tau}^{1(11)}$$
$$-\frac{\cos\beta}{2}\cos\left(\alpha+\beta\right)\left(C_{L\tau}^{1(12)}+C_{L\tau}^{1(21)}+C_{L\tau}^{2(11)}\right)-\cos\alpha\cos\beta\sin\beta\,\left(C_{L\tau}^{2(21)}+C_{L\tau}^{2(12)}+C_{L\tau}^{1(22)}\right)\Big]\,,$$
$$(2.13\text{g})$$

$$\xi_H^\tau = \frac{\cos\alpha}{\cos\beta}+\frac{v^3}{M_\tau}\frac{1}{\sqrt{2}\Lambda^2}\Big[C_{L\tau}^{2(22)}\sin^2\beta\left(-\frac{3\sin\alpha}{2}+\frac{\cos\alpha\sin\beta}{2\cos\beta}\right)-\cos\alpha\cos^2\beta\,C_{L\tau}^{1(11)}$$
$$-\frac{\cos\beta}{2}\sin\left(\alpha+\beta\right)\left(C_{L\tau}^{1(12)}+C_{L\tau}^{1(21)}+C_{L\tau}^{2(11)}\right)-\sin\alpha\cos\beta\sin\beta\,\left(C_{L\tau}^{2(21)}+C_{L\tau}^{2(12)}+C_{L\tau}^{1(22)}\right)\Big]\,,$$
$$(2.13\text{h})$$

$$\xi_A^\tau = \tan\beta+\frac{v^3}{M_\tau}\frac{1}{\sqrt{2}\Lambda^2}\Big[\frac{\sin\beta\tan\beta}{2}C_{L\tau}^{2(22)}+\sin\beta\,C_{L\tau}^{2(12)}+\frac{\cos\beta}{2}\left(C_{L\tau}^{1(12)}-C_{L\tau}^{1(21)}+C_{L\tau}^{2(11)}\right)\Big]\,,$$
$$(2.13\text{i})$$

which reduce to the usual 2HDM relations when decoupling $\Lambda\to\infty$.

3 Effective Potential at Finite Temperature

The Yukawa interactions detailed above are joined by the renormalisable (dimension 4) Higgs potential [27, 28]

$$V_{d4}(\Phi_1,\Phi_2) = m_{11}^2(\Phi_1^\dagger\Phi_1)+m_{22}^2(\Phi_2^\dagger\Phi_2)-m_{12}^2(\Phi_1^\dagger\Phi_2+\Phi_2^\dagger\Phi_1)+\lambda_1(\Phi_1^\dagger\Phi_1)^2+\lambda_2(\Phi_2^\dagger\Phi_2)^2$$
$$+\lambda_3(\Phi_1^\dagger\Phi_1)(\Phi_2^\dagger\Phi_2)+\lambda_4(\Phi_1^\dagger\Phi_2)(\Phi_2^\dagger\Phi_1)+\frac{1}{2}\lambda_5[(\Phi_1^\dagger\Phi_2)^2+(\Phi_2^\dagger\Phi_1)^2]$$
$$+\left(\lambda_6(\Phi_1^\dagger\Phi_1)+\lambda_7(\Phi_2^\dagger\Phi_2)\right)\left(\Phi_1^\dagger\Phi_2+\Phi_2^\dagger\Phi_1\right),\quad(3.1)$$

and we will focus on the CP-even case, $\lambda_6=\lambda_7=0$. Furthermore, we will only consider the soft $\mathbb{Z}_2$ breaking terms $\sim m_{12}^2$, ignoring the magenta couplings detailed above for the Yukawa interactions. We will limit our discussion to the top quark-specific interactions in the following.

The analysis of the symmetry properties at finite temperatures, see e.g. [35], requires the calculation of the one-loop effective (Coleman-Weinberg) potential at zero temperature [36] in addition to temperature corrections and associated Daisy resummation [37–39]. The potential is

most economically calculated as outlined in [37, 40], yielding

$$V_{\text{eff}}^{(1)}(\vec{\omega}, T) = \sum_{X=S,G,F} (-1)^{2s_X}(1 + 2s_X)I^X \,, \tag{3.2}$$

for a general vacuum configuration $\vec{\omega}$ in the scalar $SU(2)$ space of Eq. (2.2). Equation (3.2) sums over scalar (S), gauge field (G), fermion (F) contributions with spin quantum numbers $s_{S,G,F} = 0, 1, 1/2$ and associated one loop contributions

$$I^S = \frac{T}{2} \sum_n^{\text{Bos}} \int \frac{d^3k}{(2\pi)^3} \sum_i \left[\log \det \left(-\mathcal{D}_{S,i}^{-1} \right) \right] \,,$$

$$I^G = \frac{T}{2} \sum_n^{\text{Bos}} \int \frac{d^3k}{(2\pi)^3} \sum_i \left[\log \det \left(-\mathcal{D}_{GB,i}^{-1} \right) \right] \,, \tag{3.3}$$

$$I^F = -T \sum_n^{\text{Ferm}} \int \frac{d^3k}{(2\pi)^3} \sum_i \left[\log \det \left(-\mathcal{D}_{F,i}^{-1} \right) \right] \,,$$

where we have introduced the corresponding inverse propagators as $\mathcal{D}_X^{-1}$. At finite temperature the periodicity conditions on the two-point function require us to sum over the discrete Matsubara modes [41] in momentum space, e.g. $\mathcal{D}_S^{-1} = \omega_n^2 + \omega_k^2$ with

$$\begin{aligned} \omega_n^2 &= (2n\pi T)^2 \,, \quad n \in \mathbb{N}_0 \\ \omega_k^2 &= \boldsymbol{k}^2 + m^2 \,, \end{aligned} \tag{3.4}$$

in the imaginary time formalism. The integrals of Eq. (3.3) can be evaluated in the $\overline{\text{MS}}$ scheme

$$\begin{aligned} I_{\overline{MS}}^X &= \frac{m_X^4}{64\pi^2} \left[\log \left(\frac{m_X^2}{\mu^2} \right) - k_X \right] + \frac{T^4}{2\pi^2} J_{\pm} \left(\frac{m_X^2}{T^2} \right) \\ &= V_{\text{CW}}^X(\Phi_1, \Phi_2) + V_T^X(\Phi_1, \Phi_2) \,, \end{aligned} \tag{3.5}$$

which shows the factorisation into the temperature-independent Coleman-Weinberg (CW) contribution and a temperature-dependent contribution. The ultraviolet (UV) finite constants k_X are given by

$$k_X = \begin{cases} \frac{5}{6}, & X = G \\ \frac{3}{2}, & X = S, F \end{cases} \tag{3.6}$$

and the thermal fermionic $(+)$ and bosonic $(-)$ function $J_{\pm}$ [35, 37, 39]

$$J_{\pm}(x^2) = \int_0^\infty \mathrm{d}k \, k^2 \log \left(1 \pm e^{-\sqrt{k^2+x^2}} \right) \,. \tag{3.7}$$

The presence of Matsubara zero-modes leads to infrared problems linked to the breakdown of perturbation theory at high temperatures [42]. These infrared problems are resolved through reordering the perturbative series expansion by including thermal corrections Π to the masses, which

O_6^{111111}	$(\Phi_1^\dagger\Phi_1)^3$	O_6^{222222}	$(\Phi_2^\dagger\Phi_2)^3$
O_6^{111122}	$(\Phi_1^\dagger\Phi_1)^2(\Phi_2^\dagger\Phi_2)$	O_6^{112222}	$(\Phi_1^\dagger\Phi_1)(\Phi_2^\dagger\Phi_2)^2$
O_6^{122111}	$(\Phi_1^\dagger\Phi_2)(\Phi_2^\dagger\Phi_1)(\Phi_1^\dagger\Phi_1)$	O_6^{122122}	$(\Phi_1^\dagger\Phi_2)(\Phi_2^\dagger\Phi_1)(\Phi_2^\dagger\Phi_2)$
O_6^{121211}	$(\Phi_1^\dagger\Phi_2)^2(\Phi_1^\dagger\Phi_1)$ + h.c.	O_6^{121222}	$(\Phi_1^\dagger\Phi_2)^2(\Phi_2^\dagger\Phi_2)$ + h.c.

Table 3. Dimension-6 operators of class Φ^6 involving Φ_1 and Φ_2.

re-sums the problematic direction of the expansion parameters [35, 38, 43–46]. Concretely, we employ the Arnold-Espinosa approach [46] replacing

$$V_T \to V_T + V_{\text{daisy}}\,, \tag{3.8}$$

with

$$V_{\text{daisy}} = -\frac{T}{12\pi}\left[\sum_{i=1}^{n_{\text{Higgs}}}\left((\overline{m}_i^2)^{3/2} - (m_i^2)^{3/2}\right) + \sum_a^{n_{\text{gauge}}}\left((\overline{m}_a^2)^{3/2} - (m_a^2)^{3/2}\right)\right]\,. \tag{3.9}$$

The $\overline{m}$ masses are derived by including thermal mass corrections in the hard thermal limit. In total, the relevant 1-loop potential for our study is given by

$$V(T) = V_{\text{d4}}(T=0) + V_{\text{CW}}(T=0) + V_T(T) + V_{\text{daisy}}(T)\,. \tag{3.10}$$

The modifications of the Yukawa couplings (together with correlated four- and five-point interactions) outlined in the previous section lead to a modification of the contributions of I^F through new $m_F(\Phi_{1,2})$ contributions, thus changing the $V(T)$ away from its expectation in the $d=4$ 2HDM at $T=0$. These changes are mirrored in the temperature-dependent part alongside modifications to the plasma interactions parametrised by $\overline{m}$: Effective interactions will typically introduce new contributions to the thermal masses [47, 48], which we have included throughout (it is worth highlighting though that these do not play a relevant role for the parameter choices that we consider in this work).[4]

As done in Refs. [49, 50], it is convenient to mirror on-shell renormalisation conditions by considering additional finite counter-term contributions at $T=0$ to enforce an agreement between tree-level and one-loop effective potential minima, masses and mixing which is expressed by

$$0 = \frac{\partial}{\partial\phi_i}(V^{\text{CW}} + V^{\text{CT}})\bigg|_{\vec{\omega}_{\text{tree}}} = \frac{\partial^2}{\partial\phi_i\partial\phi_i}(V^{\text{CW}} + V^{\text{CT}})\bigg|_{\vec{\omega}_{\text{tree}}}\,. \tag{3.11}$$

Here we denote ϕ_i as the degrees of freedom in Eq. (2.2) and have further defined $\vec{\omega}_{\text{tree}}$ as the vacuum selected by Eq. (3.1), which can be aligned in our CP-even case without loss of generality in the (ζ_1, ζ_2) direction.

---

[4]Note also that the redefinition of the Yukawa interactions of Eq. (2.11) already changes the dependence $M_F(\Phi_1, \Phi_2)$ such that only in the vacuum at $T=0$ we recover the effective dimension-4 relations.
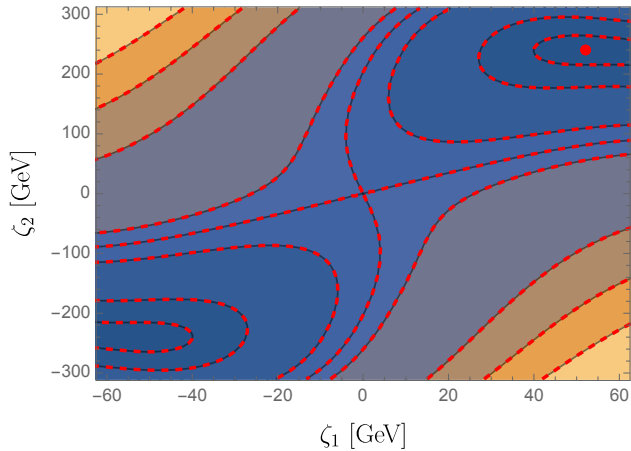
Figure 1. The 1-loop $T = 0$ vacuum structure (in arbitrary units) in the ζ_1, ζ_2 parameter space for a representative parameter choice $\lambda_1 = 2.74, \lambda_2 = 0.24, \lambda_3 = 5.53, \lambda_4 = -2.59, \lambda_5 = -2.23, (m_{11}^2, m_{22}^2, m_{12}^2) = (11212.6, -6324.6, 7738.6)$ GeV^2. This gives rise to the tree-level vacuum depicted by the red dot. The solid contours are computed from the top quark contribution to the effective potential linearised in Λ, which admits a solution to Eqs. (3.11). Overlayed in dashed contours is the full, un-truncated fermionic contribution to the effective potential employing the solution in the linearised approximation. The Wilson coefficients are chosen $C_{Qt}^{2(22)} = C_{Qt}^{1(12)} = C_{Qt}^{2(11)} = C_{Qt}^{1(22)} = C_{Qt}^{1(21)} = 4\pi, \Lambda = 1$ TeV, indicating that the linearised approximation is under good control for up to relatively large, yet perturbative Wilson coefficient choices.

When considering effective field theories, these requirements are subtle. The CW effective potential re-sums the dimension-6 EFT insertions to all orders in the Λ^{-2} expansion. In general, this means that the system of equations, Eq. (3.11), is over-constrained when only considering the renormalisation of the $d = 4$ parameters. But also including the scalar $d = 6$ interactions of Tab. 3 (see also [14, 33]) are insufficient unless the effective potential is truncated at $d = 6$. For investigations using numerical implementations such as BSMPT [51–53], this poses a technical difficulty as the expansion in Λ is no longer under analytical control: Eq. (3.11) are unattainable for general parameter choices. Analytical cross-checks show that this, however, does not lead to numerically relevant deviations for perturbative Wilson coefficient choices where we can trust our results in the first place. This is demonstrated in Fig. 1 which shows the top-quark contribution to the effective potential in the presence of top-specific Wilson coefficients.

4 Phenomenology of the Electroweak Phase Transition

4.1 Scan Methodology

The exploration of the top-EFT extended 2HDM is performed numerically using ScannerS [54–56]. We have modified the original implementation of the real 2HDM (R2HDM) to include the operators given in Tab. 2. Furthermore, we modified accordingly the code HDECAY [57–59] for the computation of the QCD corrected branching ratios of all scalar particles. We choose the 2HDM mass spectrum, $\tan \beta$, the soft-breaking m_{12}^2, the coupling of the heavy CP-even Higgs boson to massive gauge bosons c_{HVV}, as well as the corresponding Wilson coefficients (setting $\Lambda = 1$ TeV) as input parameters.

m_h [GeV]	m_H [GeV]	m_A [GeV]	$m_{H^\pm}$ [GeV]	$\tan\beta$	c_{HVV}	m_{12}^2 [GeV^2]
125.09	130...3000	30...3000	800...3000	0.8...30	-0.3...1.0	$10^{-5}...10^7$

Table 4. Scan ranges of the 2HDM input parameters.

The light Higgs boson is selected to have a mass of

$$m_h = 125.09 \text{ GeV} \tag{4.1}$$

and behave SM-like. Points are generated from random numbers and their consistency with phenomenological constraints is checked by `ScannerS` using `HiggsBounds` [60–63] and `HiggsSignals` [64, 65]. Flavour constraints are taken into account through consistency with $\mathcal{R}_b$ [66, 67] and $B \to X_s\gamma$ [67–72]. Given the Yukawa type II considered here, the charged Higgs mass is constrained to be $m_{H^\pm} \geq 800$ GeV [72], virtually independent of $\tan\beta$.[5] The input parameters' minimum and maximum allowed ranges are provided in Tab. 4. The imposed limit on the charged Higgs mass effectively removes phenomenological sensitivity to this state, and we will focus on modifications of the neutral states, which are much more accessible at the LHC. The coupling modifiers analogous to Eq. (2.13) are given in appendix A for completeness.

The experimentally and theoretically validated parameter points found with `ScannerS` are further investigated with our code `BSMPT` [51–53]. Our scan methodology works like follows:

1. We scan for a dim-4 point (all Wilson coefficients $C_{Qt}^i = 0$) that is in agreement with theoretical and experimental constraints with `ScannerS` and whose strength of the electroweak phase transition is $\xi_c^{d4} < 1$ (no SFOEWPT yet) which we check with `BSMPT`.

   For each dim-6 Wilson coefficient direction C_{Qt}^i we then check the following:

2. The selected dim-6 direction is varied with $C_{Qt}^i = \pm 0.01$ and we evaluate the response in ξ_c^{d6} by tracing the phases in a range of $T_c^{d4} \pm 15$ GeV around the dim-4 critical temperature T_c^{d4}.[6] For the minimum phase tracing, we use the new minimum tracing algorithms of `BSMPTv3` [53].

3. From the results for $\xi_{c,\pm 0.01}^{d6}$, we make a prediction for the Wilson coefficient $C_{Qt}^{i,\text{SFOEWPT}}$ leading to an SFOEWPT, assuming a linear response.

4. The prediction is checked with `ScannerS` including special focus on the $h_{125}t\bar{t}$ coupling. If the predicted point is found to be valid, we derive ξ_c^{d6} with `BSMPTv3` as described in step 2. Here, we adjust the temperature ranges for minima tracing iteratively.

5. We keep the point as a valid linear response dim-6 SFOEWPT point if $\xi_c^{d6,\text{ pred}}$ differs from $\xi_c^{\text{SFOEWPT}} = 1$ by less than 1 %. For relative differences above 10 % we discard the point due to

---

[5]The bound on $m_{H^\pm}$ is currently subject to investigation given the recent results by Belle-II [72–74].

[6]Due to our lack of analytical control over the Λ^{-1} expansion, our non-linearized calculation manifests itself into small deviations from the EW minimum at $T = 0$ GeV, as well as small deviations from EW symmetry restoration at $T = 300$ GeV. Because we analytically found them to be numerically irrelevant for perturbative Wilson coefficient choices, we are only interested in studying the impact of C_{Qt}^i on the behaviour of the false and true coexisting minima phases around the dim-4 critical temperature.

m_h [GeV]	m_H [GeV]	m_A [GeV]	$m_{H^\pm}$ [GeV]	$\tan\beta$	c_{HVV}	m_{12}^2 [GeV^2]
125.09	683	872	868	1.658	0.00350	205007

T_c^{d4} [GeV]	$v(T_c)^{\mathrm{d4}}$ [GeV]	ξ_c^{d4}
226.29	215.69	0.95

**Table 5**. Input parameters of the benchmark point used for Fig. 2.
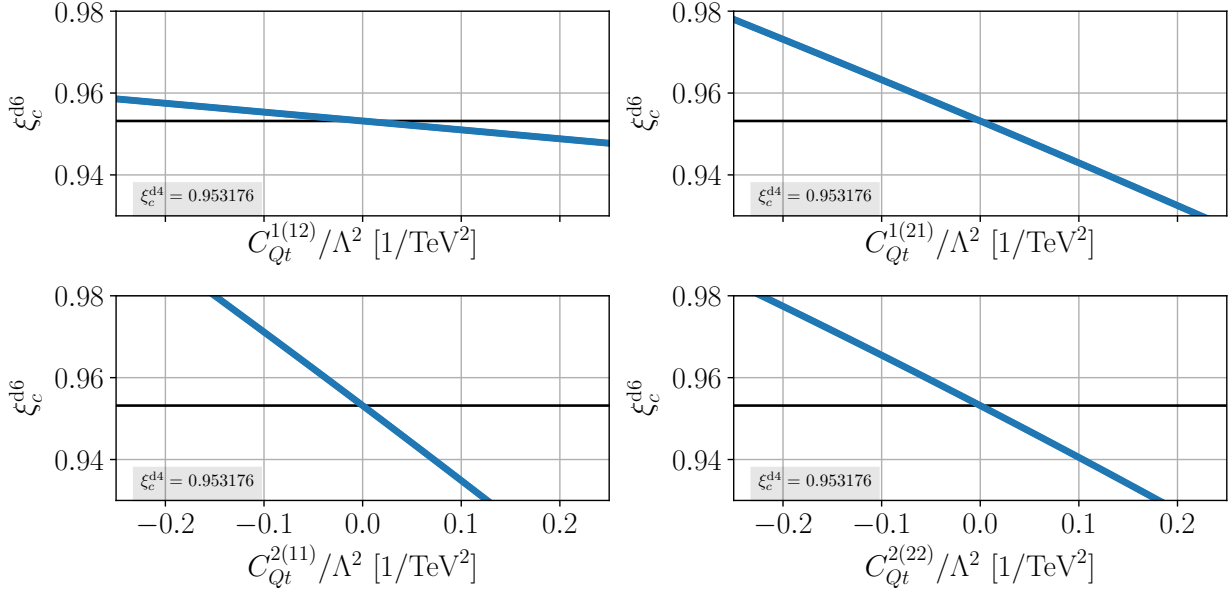
Figure 2. Response in ξ_c^{d6} (in blue) in all Wilson coefficient directions separately for a representative parameter point of the Type-2 2HDM with $\xi_c^{\mathrm{d4}} \simeq 0.95$. The dim-4 ξ_c^{d4} is marked as a black line. The displayed point is given in Table 5.

showing a non-linear response that violates our assumption of perturbative Wilson coefficient choices. For $1\% < |1 - \xi_c^{\mathrm{d6, \, pred}}| < 10\%$ we make an updated linearised prediction for the dim-6 Wilson coefficient strength needed for an SFOEWPT based on the previous iteration

$$C_{Qt}^{i,\mathrm{SFOEWPT}} = C_{Qt}^{i,\mathrm{prev}} \cdot \left(\frac{1 - \xi_c^{\mathrm{d4}}}{\xi_c^{\mathrm{d6, \, prev}} - \xi_c^{\mathrm{d4}}} \right) \tag{4.2}$$

and repeat steps 4. and 5. until a valid linear-response dim-6 SFOEWPT point is found or the point has to be discarded due to detected non-linearities.

In Fig. 2 we show the detailed response in ξ_c^{d6} for one picked exemplary linear-response parameter point. The point is given in Tab. 5 in detail. As can be seen in these plots the generic response to EFT parameter modifications is linear. This means that although the potential receives non-linear contributions from the EFT correlation changes, these formally higher-order modifications are not relevant within the region that we study in this work. These results can therefore be taken as a consistency check of the dimension 6 approach outlined in the previous section.
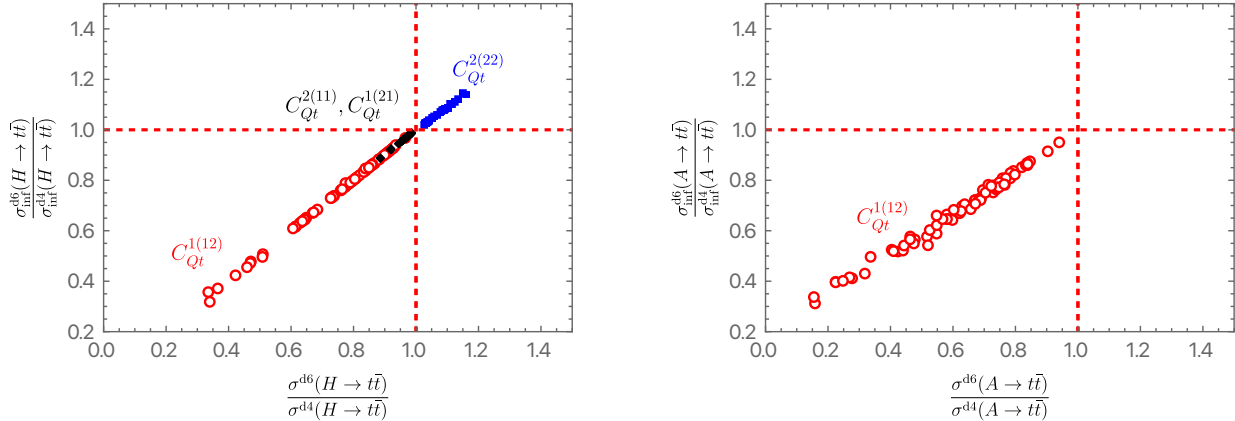
Figure 3. Correlation of dimension-6 modified signal cross sections σ^{d6} relative to their dimension-4 2HDM expectation σ^{d4}. The cross sections $\sigma^{d4}_{inf}, \sigma^{d6}_{inf}$ include interference effects with other signal contributions (e.g. propagating A, h contributions in case of H production) in the 2HDM as well as, most importantly, interference effects with QCD-induced $t\bar{t}$ production. We include points that are characterised by $\xi^{d4}_c < 0.96$.

4.2 Results and Implications of a Top-Philic SFOEWPT

Small modifications of the top interactions can have a sizeable impact on Higgs signal strengths

$$\mu(h \to XY) = \frac{[\sigma(h) \times \text{BR}(h \to XY)]^{d6}}{[\sigma(h) \times \text{BR}(h \to XY)]^{d4}} \tag{4.3}$$

where $\sigma(h)$ is the light Higgs production cross section and $\text{BR}(h \to XY)$ the branching ratio into the final state $h \to XY$. In particular, the branching ratio of the $h \to \gamma\gamma$ decay, which is already significantly constrained and will provide a formidable avenue to constrain this direction in the future, limits the freedom of BSM interactions. The coupling modifier of the 2HDM can move quickly away as a function of the Wilson coefficients from the alignment limit that is preferred by the increasingly SM-consistent outcome of Higgs measurements at the LHC. This becomes particularly clear in a dedicated scan of *individual* operator directions of Tab. 2. Indeed we find the Higgs signal strength constraints that are part of our workflow, Sec. 4.1, limit our freedom of Wilson coefficients, highlighting scan points that achieve $\xi^{d6}_c > 1$ from distances $1 - \xi^{d4}_c \simeq 10\%$, i.e. we can only bridge small d4 phase transition distances without violating signal strength constraints. This consistency with the SM outcome naturally moves us to a parameter domain where EFT modifications can be trusted.

In parallel, we require a priori significant Yukawa-sector modifications to enable a stronger phase transition in comparison with the SM alone (see also the discussion in Ref. [15] in the context of a different model).[7] Parametric freedom in signal strength constraints (that are included in our scan as described in Sec. 4.1) can be achieved for mixing angles that reduce the sensitivity to a particular

---

[7]We note at this point that requiring $\xi^{d6}_c = 1$ as a numerical value does not automatically guarantee an SFOEWPT. What we are interested in predominantly in the following are the phenomenological consequences at the LHC that are implied by "gradients" in $\xi^{d4}_c \to \xi^{d6}_c \gtrsim 1$. This enables us to qualitatively understand exclusion constraints or the lack of new physics signatures through the lens of overcoming the shortfalls of the 2HDM type II.

Wilson coefficient for the 125 GeV Higgs.[8] Compatibility of the 2HDM predictions with the currently observed consistency of $h = H_{\text{SM}}$ favours regions of $\tan\beta \sim \mathcal{O}(1)$ at a coupling modifier $\xi_h^t \simeq 1$, Eq. (2.13a), isolating the alignment limit $\cos\alpha \simeq \sin\beta$ in the Yukawa sector. For these parameter choices, $\sin\alpha < 0$ in our conventions, so that the negative Wilson coefficient choices that drive $\xi_c^{\text{d6}} \to 1$ are correlated with slightly enhanced coupling modifiers ξ_h^t. This increases the thermal contribution to the Higgs potential from the lightest and therefore most relevant degrees of freedom for the thermodynamical problem at hand.

In case of the $O_{Qt}^{1(12)}$ interactions, the correlated modification for the heavy H, Eq. (2.13b), is then a reduced coupling strength $|\xi_H^t(C_{Qt}^{1(12)})| < |\xi_H^t(C_{Qt}^{1(12)} = 0)|$, which is mirrored by the CP-odd state as $\tan\beta > 0$, Eq. (2.13c). The new physics operators can modify the h coupling strengths at the order of 10% given current Higgs constraints, and a sizeable Wilson coefficient to drive the EWPT requires suppression to maintain consistency with light Higgs observations. Depending on the particular regions of parameter space where $\xi_c^{\text{d6}} \simeq 1$ and agreement with available data can be achieved in the scan detailed above, an interesting phenomenological implication arises, which especially highlights $O_{Qt}^{1(12)}$. Heavy physics parametrised by $C_{Qt}^{1(12)}$ that points towards an SFOEWPT is correlated with an underproduction of the additional Higgs bosons in the 2HDM in the dominant gluon fusion channels $gg \to H/A \to t\bar{t}$, Fig. 3. The relative reduction due to angular suppression of the Wilson coefficient to maintain consistency with h data is not given for the heavy states whose phenomenology therefore significantly departs from the d4 2HDM expectation.

Contrary to the $O_{Qt}^{1(12)}$, the structure of $O_{Qt}^{2(22)}$ is such that

$$\left.\frac{\xi_H^{t,\text{d6}}}{\xi_h^{t,\text{d6}}}\right|_{O_{Qt}^{2(22)}} = \left.\frac{\xi_H^{t,\text{d4}}}{\xi_h^{t,\text{d4}}}\right|_{O_{Qt}^{2(22)}} = \tan\alpha \,, \tag{4.4}$$

$$\left.\frac{\xi_h^{t,\text{d6}}}{\xi_h^{t,\text{d4}}}\right|_{O_{Qt}^{2(22)}} = \left.\frac{\xi_H^{t,\text{d6}}}{\xi_H^{t,\text{d4}}}\right|_{O_{Qt}^{2(22)}} = 1 - C_{Qt}^{2(22)} \frac{v^2}{\Lambda^2} \frac{v}{\sqrt{2}M_t} \sin^3\beta \,. \tag{4.5}$$

Due to the vacuum structure of this operator, the h, and H phenomenology modifications are fully correlated, independent of the size of the Wilson coefficient. An enhanced strength of the phase transition then manifests itself through a dedicated pattern in strengths of H vs h interactions that can depart from the 2HDM d4 expectation at 20% enhancement whilst the CP odd Higgs boson interactions are unchanged to leading approximation.

Interactions related to $O_{Qt}^{1(21)}, O_{Qt}^{2(11)}$ impact the neutral Higgs sector identically, and therefore the phenomenology is correlated. We, therefore, show their results combined in Fig. 3. The qualitative picture is similar to $O_{Qt}^{1(12)}$, however, as ξ_c^{d6} is more sensitive to the Wilson coefficient in this case. This can be seen, e.g., in the steeper gradient displayed for $C_{Qt}^{1(21)}, C_{Qt}^{2(11)}$ for the sample parameter point in Fig. 2 compared to $C_{Qt}^{1(12)}$. Hence, the quantitative impact is reduced.

It is well-known that these searches are limited by accidental signal background interference [75], however, the reduction in signal rate does not qualitatively change the observed outcome on which the model-dependent investigations at the LHC (e.g. [76, 77]) are based. This means that when

---

[8]The operator $\sim C_{Qt}^{1(21)}$ is particularly worth highlighting here as it is the only $\mathbb{Z}_2$ symmetry conserving operator that modifies the interactions with the CP-odd scalar, thus offering additional phenomenological handles at the LHC.
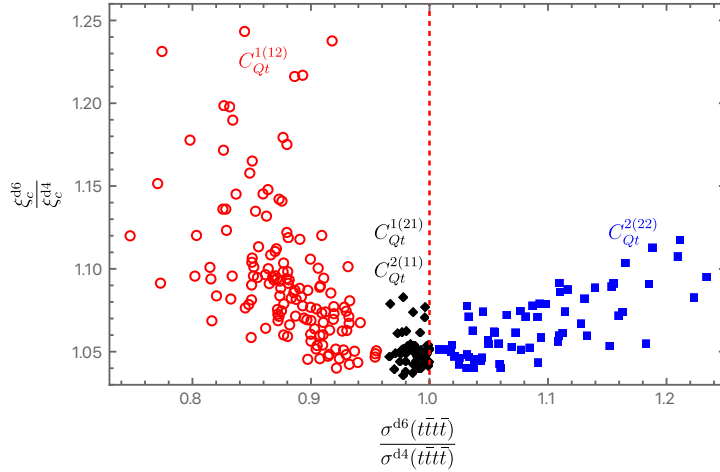
Figure 4. Correlation of the modified production cross-section for $pp \to t\bar{t}t\bar{t}$ (σ^{d6}/σ^{d4}) with modification in the strength of the phase transition (ξ_c^{d6}/ξ_c^{d4}). The corresponding contributions for the different effective operators are shown and the points are chosen with $\xi_c^{d4} < 0.96$.

considering the correlation changes anticipated from dimension-6 deformations of the 2HDM type II, the established experimental strategies remain valid. In Fig. 4, we also show the implications for four top final states $pp \to t\bar{t}t\bar{t}$ (which includes all Higgs contributions in s and t channels). This process has been motivated as an additional (interference-robust) tool to constrain or observe new physics [78–82] (see also the recent LHC results of [83, 84]). The implications for the four top final states are identical to $gg \to H/A \to t\bar{t}$, cf. Fig. 3.

What is perhaps most important at this point in the LHC programme is that when we consider the aforementioned correlation changes that address cosmological shortcomings of the 2HDM at face value, the LHC sensitivity is currently *overestimated*, predominantly for $C_{Qt}^{1(12)}$, for which also the CP-odd scalar has a suppressed phenomenology (such states are abundantly produced compared to the CP-even scalar due to a different threshold behavior [85]). This alludes to the tantalising possibility that the 2HDM type-II could indeed be realised at the TeV scale with additional heavier physics modifying the expected correlations in such a way that the current constraints are weakened, yet shortfalls of the SM (and the 2HDM) are cured. This constitutes an exciting prospect for the LHC Run-3.

5   Conclusions

The requirement of a strong first-order electroweak phase transition is a strong hint for a source of new physics beyond the Standard Model. Yet, current analyses at the high-energy regime of the LHC seem to indicate that electroweak symmetry breaking is well-described by the ad-hoc implementation of the SM. On the one hand, these recent observations imply mounting pressure on BSM scenarios such as the 2HDM type II that we have considered in this work. On the other hand, consistency with the SM hypothesis could indicate top-philic cancellations as part of high-scale physics which is well-expressed using effective field theory in the intermediate energy regime between the 2HDM

and its extension. Taking this as motivation we analyse Yukawa sector modifications as potential sources to facilitate a strong first-order electroweak phase transition in the early universe. While such cancellations reproduce the alignment limit of the 2HDM to maintain consistency with current Higgs data they show up as characteristic deformations of the 2HDM heavy states' phenomenology. Not only is this qualitatively different from the scalar sector deformations discussed in Ref. [14], but the implied phenomenological consequences for the LHC are encouraging: Current analysis strategies, whilst remaining robust strategies to lead to discoveries in the future, can overestimate the new physics potential of exotic Higgs searches in the 2HDM when its deformations to an SFOEWPT are considered as a result of $O_{Qt}^{1(12)}$.

Acknowledgements

A EFT Modifications of Charged Higgs Interactions

With $\Psi^2\Phi^3$ insertions, the dimension-4 charged Higgs couplings to the fermions Eq. (2.7) get modified. For the third-generation fermions, these modifications are

$$
\begin{aligned}
\mathcal{L}_{\text{charged}}^{\text{dim-6}} = \\
\frac{\sqrt{2}}{v} \Bigg[\bar{t} \, \bigg\{ &\bigg(M_b \, V_{tb} \tan\beta + \frac{v^3 \sin\beta}{2\sqrt{2}\Lambda^2} \Big(C_{Qb}^{2(12)} + C_{Qb}^{2(21)} + C_{Qb}^{2(11)} \cot\beta + C_{Qb}^{2(22)} \tan\beta \Big) \bigg) \mathrm{P_R} \\
+ &V_{tb} \bigg(M_t \cot\beta + \frac{v^3 \cos\beta}{2\sqrt{2}\Lambda^2} \Big(C_{Qt}^{1(12)} + C_{Qt}^{1(21)} + C_{Qt}^{1(11)} \cot\beta + C_{Qt}^{1(22)} \tan\beta \Big) \bigg) \mathrm{P_L} \bigg\} b \, H^+ \\
+ \bar{\nu}_\tau &\bigg(M_\tau \tan\beta + \frac{v^3 \sin\beta}{2\sqrt{2}\Lambda^2} \Big(C_{L\tau}^{2(12)} + C_{L\tau}^{2(21)} + C_{L\tau}^{2(11)} \cot\beta + C_{L\tau}^{2(22)} \tan\beta \Big) \bigg) \mathrm{P_R} \, \tau \, H^+ + \text{h.c.} \Bigg].
\end{aligned}
$$

(A.1)

Again for $\Lambda \to \infty$, the standard 2HDM relations of Eq. (2.7) are recovered.

References

[1] M. Baak, M. Goebel, J. Haller, A. Hoecker, D. Kennedy, R. Kogler et al., *The Electroweak Fit of the Standard Model after the Discovery of a New Boson at the LHC*, *Eur. Phys. J. C* **72** (2012) 2205, [1209.2716].

[2] G. Degrassi, S. Di Vita, J. Elias-Miro, J. R. Espinosa, G. F. Giudice, G. Isidori et al., *Higgs mass and vacuum stability in the Standard Model at NNLO*, *JHEP* **08** (2012) 098, [1205.6497].

[3] A. V. Bednyakov, B. A. Kniehl, A. F. Pikelner and O. L. Veretin, *Stability of the Electroweak Vacuum: Gauge Independence and Advanced Precision*, *Phys. Rev. Lett.* **115** (2015) 201802, [`1507.08833`].

[4] U. Baur, T. Plehn and D. L. Rainwater, *Measuring the Higgs Boson Self Coupling at the LHC and Finite Top Mass Matrix Elements*, *Phys. Rev. Lett.* **89** (2002) 151801, [`hep-ph/0206024`].

[5] C. Englert, M. McCullough and M. Spannowsky, *Gluon-initiated associated production boosts Higgs physics*, *Phys. Rev. D* **89** (2014) 013013, [`1310.4828`].

[6] A. D. Sakharov, *Violation of CP Invariance, C asymmetry, and baryon asymmetry of the universe*, *Pisma Zh. Eksp. Teor. Fiz.* **5** (1967) 32–35.

[7] C. Englert, P. Galler, A. Pilkington and M. Spannowsky, *Approaching robust EFT limits for CP-violation in the Higgs sector*, *Phys. Rev. D* **99** (2019) 095007, [`1901.05982`].

[8] B. Bortolato, J. F. Kamenik, N. Košnik and A. Smolkovič, *Optimized probes of CP -odd effects in the $t\bar{t}h$ process at hadron colliders*, *Nucl. Phys. B* **964** (2021) 115328, [`2006.13110`].

[9] R. K. Barman, D. Gonçalves and F. Kling, *Machine learning the Higgs boson-top quark CP phase*, *Phys. Rev. D* **105** (2022) 035023, [`2110.07635`].

[10] T. D. Lee, *A Theory of Spontaneous T Violation*, *Phys. Rev. D* **8** (1973) 1226–1239.

[11] G. C. Branco, P. M. Ferreira, L. Lavoura, M. N. Rebelo, M. Sher and J. P. Silva, *Theory and phenomenology of two-Higgs-doublet models*, *Phys. Rept.* **516** (2012) 1–102, [`1106.0034`].

[12] D. Fontes, M. Mühlleitner, J. C. Romão, R. Santos, J. a. P. Silva and J. Wittbrodt, *The C2HDM revisited*, *JHEP* **02** (2018) 073, [`1711.09419`].

[13] P. Basler, S. Dawson, C. Englert and M. Mühlleitner, *Showcasing HH production: Benchmarks for the LHC and HL-LHC*, *Phys. Rev. D* **99** (2019) 055048, [`1812.03542`].

[14] Anisha, L. Biermann, C. Englert and M. Mühlleitner, *Two Higgs doublets, effective interactions and a strong first-order electroweak phase transition*, *JHEP* **08** (2022) 091, [`2204.06966`].

[15] I. Baldes, T. Konstandin and G. Servant, *A first-order electroweak phase transition from varying Yukawas*, *Phys. Lett. B* **786** (2018) 373–377, [`1604.04526`].

[16] P. Basler, M. Krause, M. Muhlleitner, J. Wittbrodt and A. Wlotzka, *Strong First Order Electroweak Phase Transition in the CP-Conserving 2HDM Revisited*, *JHEP* **02** (2017) 121, [`1612.04086`].

[17] O. Atkinson, M. Black, A. Lenz, A. Rusov and J. Wynne, *Cornering the Two Higgs Doublet Model Type II*, *JHEP* **04** (2022) 172, [`2107.05650`].

[18] O. Atkinson, M. Black, C. Englert, A. Lenz, A. Rusov and J. Wynne, *The flavourful present and future of 2HDMs at the collider energy frontier*, *JHEP* **11** (2022) 139, [`2202.08807`].

[19] O. Atkinson, M. Black, C. Englert, A. Lenz and A. Rusov, *MUonE, muon g-2 and electroweak precision constraints within 2HDMs*, *Phys. Rev. D* **106** (2022) 115031, [`2207.02789`].

[20] S. Das Bakshi, J. Chakrabortty and S. K. Patra, *CoDEx: Wilson coefficient calculator connecting SMEFT to UV theory*, *Eur. Phys. J. C* **79** (2019) 21, [`1808.04403`].

[21] A. Carmona, A. Lazopoulos, P. Olgoso and J. Santiago, *Matchmakereft: automated tree-level and one-loop matching*, *SciPost Phys.* **12** (2022) 198, [`2112.10787`].

[22] J. Fuentes-Martín, M. König, J. Pagès, A. E. Thomsen and F. Wilsch, *A proof of concept for matchete: an automated tool for matching effective theories*, *Eur. Phys. J. C* **83** (2023) 662, [`2212.04510`].

[23] T. Cohen, X. Lu and Z. Zhang, *Functional Prescription for EFT Matching, JHEP* **02** (2021) 228, [2011.02484].

[24] S. Dawson, D. Fontes, S. Homiller and M. Sullivan, *Role of dimension-eight operators in an EFT for the 2HDM, Phys. Rev. D* **106** (2022) 055012, [2205.01561].

[25] S. Dawson, D. Fontes, C. Quezada-Calonge and J. J. Sanz-Cillero, *Matching the 2HDM to the HEFT and the SMEFT: Decoupling and perturbativity, Phys. Rev. D* **108** (2023) 055034, [2305.07689].

[26] M. Postma and G. White, *Cosmological phase transitions: is effective field theory just a toy?, JHEP* **03** (2021) 280, [2012.03953].

[27] J. F. Gunion, H. E. Haber, G. L. Kane and S. Dawson, *The Higgs Hunter's Guide*, vol. 80. Perseus Publishing, 2000.

[28] J. F. Gunion and H. E. Haber, *The CP conserving two Higgs doublet model: The Approach to the decoupling limit, Phys. Rev. D* **67** (2003) 075019, [hep-ph/0207010].

[29] D. Gonçalves, A. Kaladharan and Y. Wu, *Gravitational waves, bubble profile, and baryon asymmetry in the complex 2HDM, Phys. Rev. D* **108** (2023) 075010, [2307.03224].

[30] B. Grzadkowski, M. Iskrzynski, M. Misiak and J. Rosiek, *Dimension-Six Terms in the Standard Model Lagrangian, JHEP* **10** (2010) 085, [1008.4884].

[31] A. Crivellin, M. Ghezzi and M. Procura, *Effective Field Theory with Two Higgs Doublets, JHEP* **09** (2016) 160, [1608.00975].

[32] S. Karmakar and S. Rakshit, *Higher dimensional operators in 2HDM, JHEP* **10** (2017) 048, [1707.00716].

[33] Anisha, S. Das Bakshi, J. Chakrabortty and S. Prakash, *Hilbert Series and Plethystics: Paving the path towards 2HDM- and MLRSM-EFT, JHEP* **09** (2019) 035, [1905.11047].

[34] U. Banerjee, J. Chakrabortty, S. Prakash and S. U. Rahaman, *Characters and group invariant polynomials of (super)fields: road to "Lagrangian", Eur. Phys. J. C* **80** (2020) 938, [2004.12830].

[35] M. Quiros, *Field theory at finite temperature and phase transitions, Helv. Phys. Acta* **67** (1994) 451–583.

[36] S. R. Coleman and E. J. Weinberg, *Radiative Corrections as the Origin of Spontaneous Symmetry Breaking, Phys. Rev. D* **7** (1973) 1888–1910.

[37] L. Dolan and R. Jackiw, *Symmetry Behavior at Finite Temperature, Phys. Rev. D* **9** (1974) 3320–3341.

[38] M. E. Carrington, *The Effective potential at finite temperature in the Standard Model, Phys. Rev. D* **45** (1992) 2933–2944.

[39] M. Quiros, *Finite temperature field theory and phase transitions*, in *ICTP Summer School in High-Energy Physics and Cosmology*, pp. 187–259, 1, 1999. hep-ph/9901312.

[40] R. Jackiw, *Functional evaluation of the effective potential, Phys. Rev. D* **9** (1974) 1686.

[41] T. Matsubara, *A New approach to quantum statistical mechanics, Prog. Theor. Phys.* **14** (1955) 351–378.

[42] S. Weinberg, *Gauge and Global Symmetries at High Temperature, Phys. Rev. D* **9** (1974) 3357–3378.

[43] R. R. Parwani, *Resummation in a hot scalar field theory, Phys. Rev. D* **45** (1992) 4695, [hep-ph/9204216].

[44] P. B. Arnold, *Phase transition temperatures at next-to-leading order, Phys. Rev. D* **46** (1992) 2628–2635, [hep-ph/9204228].

[45] J. I. Kapusta and C. Gale, *Finite-temperature field theory: Principles and applications.* Cambridge Monographs on Mathematical Physics. Cambridge University Press, 2011, 10.1017/CBO9780511535130.

[46] P. B. Arnold and O. Espinosa, *The Effective potential and first order phase transitions: Beyond leading-order*, *Phys. Rev. D* **47** (1993) 3546, [hep-ph/9212235].

[47] D. Bodeker, L. Fromme, S. J. Huber and M. Seniuch, *The Baryon asymmetry in the standard model with a low cut-off*, *JHEP* **02** (2005) 026, [hep-ph/0412366].

[48] D. Croon, O. Gould, P. Schicho, T. V. I. Tenkanen and G. White, *Theoretical uncertainties for cosmological first-order phase transitions*, *JHEP* **04** (2021) 055, [2009.10080].

[49] P. Basler, M. Mühlleitner and J. Müller, *Electroweak Phase Transition in Non-Minimal Higgs Sectors*, *JHEP* **05** (2020) 016, [1912.10477].

[50] P. Basler, M. Mühlleitner and J. Müller, *Electroweak Baryogenesis in the CP-Violating Two-Higgs Doublet Model*, 2108.03580.

[51] P. Basler and M. Mühlleitner, *BSMPT (Beyond the Standard Model Phase Transitions): A tool for the electroweak phase transition in extended Higgs sectors*, *Comput. Phys. Commun.* **237** (2019) 62–85, [1803.02846].

[52] P. Basler, M. Mühlleitner and J. Müller, *BSMPT v2 a tool for the electroweak phase transition and the baryon asymmetry of the universe in extended Higgs Sectors*, *Comput. Phys. Commun.* **269** (2021) 108124, [2007.01725].

[53] L. Biermann, M. Mühlleitner, R. Santos and J. Viana, *BSMPT v3, to appear*.

[54] R. Coimbra, M. O. P. Sampaio and R. Santos, *ScannerS: Constraining the phase diagram of a complex scalar singlet at the LHC*, *Eur. Phys. J. C* **73** (2013) 2428, [1301.2599].

[55] R. Costa, R. Guedes, M. O. P. Sampaio and R. Santos, SCANNERS *project*, October, 2014.

[56] M. Mühlleitner, M. O. P. Sampaio, R. Santos and J. Wittbrodt, *ScannerS: parameter scans in extended scalar sectors*, *Eur. Phys. J. C* **82** (2022) 198, [2007.02985].

[57] A. Djouadi, J. Kalinowski and M. Spira, *HDECAY: A Program for Higgs boson decays in the standard model and its supersymmetric extension*, *Comput. Phys. Commun.* **108** (1998) 56–74, [hep-ph/9704448].

[58] R. Harlander, M. Mühlleitner, J. Rathsman, M. Spira and O. Stål, *Interim recommendations for the evaluation of Higgs production cross sections and branching ratios at the LHC in the Two-Higgs-Doublet Model*, 1312.5571.

[59] HDECAY collaboration, A. Djouadi, J. Kalinowski, M. Muehlleitner and M. Spira, *HDECAY: Twenty$_{++}$ years after*, *Comput. Phys. Commun.* **238** (2019) 214–231, [1801.09506].

[60] P. Bechtle, O. Brein, S. Heinemeyer, G. Weiglein and K. E. Williams, *HiggsBounds: Confronting Arbitrary Higgs Sectors with Exclusion Bounds from LEP and the Tevatron*, *Comput. Phys. Commun.* **181** (2010) 138–167, [0811.4169].

[61] P. Bechtle, O. Brein, S. Heinemeyer, G. Weiglein and K. E. Williams, *HiggsBounds 2.0.0: Confronting Neutral and Charged Higgs Sector Predictions with Exclusion Bounds from LEP and the Tevatron*, *Comput. Phys. Commun.* **182** (2011) 2605–2631, [1102.1898].

[62] P. Bechtle, O. Brein, S. Heinemeyer, O. Stål, T. Stefaniak, G. Weiglein et al., HiggsBounds − 4: *Improved Tests of Extended Higgs Sectors against Exclusion Bounds from LEP, the Tevatron and the LHC*, *Eur. Phys. J. C* **74** (2014) 2693, [1311.0055].

[63] P. Bechtle, D. Dercks, S. Heinemeyer, T. Klingl, T. Stefaniak, G. Weiglein et al., *HiggsBounds-5: Testing Higgs Sectors in the LHC 13 TeV Era*, *Eur. Phys. J. C* **80** (2020) 1211, [2006.06007].

[64] P. Bechtle, S. Heinemeyer, O. Stål, T. Stefaniak and G. Weiglein, *HiggsSignals: Confronting arbitrary Higgs sectors with measurements at the Tevatron and the LHC*, *Eur. Phys. J. C* **74** (2014) 2711, [1305.1933].

[65] P. Bechtle, S. Heinemeyer, T. Klingl, T. Stefaniak, G. Weiglein and J. Wittbrodt, *HiggsSignals-2: Probing new physics with precision Higgs measurements in the LHC 13 TeV era*, *Eur. Phys. J. C* **81** (2021) 145, [2012.09197].

[66] H. E. Haber and H. E. Logan, *Radiative corrections to the Z b anti-b vertex and constraints on extended Higgs sectors*, *Phys. Rev. D* **62** (2000) 015011, [hep-ph/9909335].

[67] O. Deschamps, S. Descotes-Genon, S. Monteil, V. Niess, S. T'Jampens and V. Tisserand, *The Two Higgs Doublet of Type II facing flavour physics data*, *Phys. Rev. D* **82** (2010) 073012, [0907.5135].

[68] F. Mahmoudi and O. Stal, *Flavor constraints on the two-Higgs-doublet model with general Yukawa couplings*, *Phys. Rev. D* **81** (2010) 035016, [0907.1791].

[69] T. Hermann, M. Misiak and M. Steinhauser, $\bar{B} \to X_s\gamma$ *in the Two Higgs Doublet Model up to Next-to-Next-to-Leading Order in QCD*, *JHEP* **11** (2012) 036, [1208.2788].

[70] M. Misiak et al., *Updated NNLO QCD predictions for the weak radiative B-meson decays*, *Phys. Rev. Lett.* **114** (2015) 221801, [1503.01789].

[71] M. Misiak and M. Steinhauser, *Weak radiative decays of the B meson and bounds on $M_{H^\pm}$ in the Two-Higgs-Doublet Model*, *Eur. Phys. J. C* **77** (2017) 201, [1702.04571].

[72] M. Misiak, A. Rehman and M. Steinhauser, *Towards $\overline{B} \to X_s\gamma$ at the NNLO in QCD without interpolation in m_c*, *JHEP* **06** (2020) 175, [2002.01548].

[73] Belle-II collaboration, F. Abudinén et al., *Measurement of the photon-energy spectrum in inclusive $B \to X_s\gamma$ decays identified using hadronic decays of the recoil B meson in 2019-2021 Belle II data*, 2210.10220.

[74] M. Steinhauser, *private communication*.

[75] K. J. F. Gaemers and F. Hoogeveen, *Higgs Production and Decay Into Heavy Flavors With the Gluon Fusion Mechanism*, *Phys. Lett. B* **146** (1984) 347–349.

[76] CMS collaboration, A. M. Sirunyan et al., *Search for heavy Higgs bosons decaying to a top quark pair in proton-proton collisions at $\sqrt{s} = 13$ TeV*, *JHEP* **04** (2020) 171, [1908.01115].

[77] ATLAS collaboration, M. Aaboud et al., *Search for Heavy Higgs Bosons A/H Decaying to a Top Quark Pair in pp Collisions at $\sqrt{s} = 8$ TeV with the ATLAS Detector*, *Phys. Rev. Lett.* **119** (2017) 191803, [1707.06025].

[78] E. Alvarez, D. A. Faroughy, J. F. Kamenik, R. Morales and A. Szynkman, *Four tops for LHC*, *Nucl. Phys. B* **915** (2017) 19–43, [1611.05032].

[79] E. Alvarez, A. Juste and R. M. S. Seoane, *Four-top as probe of light top-philic New Physics*, *JHEP* **12** (2019) 080, [1910.09581].

[80] S. Kanemura, H. Yokoya and Y.-J. Zheng, *Searches for additional Higgs bosons in multi-top-quarks events at the LHC and the International Linear Collider*, *Nucl. Phys. B* **898** (2015) 286–300, [1505.01089].

[81] F. Blekman, F. Déliot, V. Dutta and E. Usai, *Four-top quark physics at the LHC*, *Universe* **8** (2022) 638, [2208.04085].

[82] Anisha, O. Atkinson, A. Bhardwaj, C. Englert, W. Naskar and P. Stylianou, *BSM reach of four-top production at the LHC*, *Phys. Rev. D* **108** (2023) 035001, [2302.08281].

[83] ATLAS collaboration, G. Aad et al., *Observation of four-top-quark production in the multilepton final state with the ATLAS detector*, *Eur. Phys. J. C* **83** (2023) 496, [2303.15061].

[84] CMS collaboration, A. Hayrapetyan et al., *Observation of four top quark production in proton-proton collisions at $\sqrt{s} = 13$ TeV*, 2305.13439.

[85] A. Djouadi, *The Anatomy of electro-weak symmetry breaking. I: The Higgs boson in the standard model*, *Phys. Rept.* **457** (2008) 1–216, [hep-ph/0503172].